INSTITUT CATALÀ DE CIÈNCIES DEL CLIMA

Institut Català de Ciències del Clima

C/ Doctor Trueta, 203
Barcelona, 08005
Phone: +34 93 309 7600
Web: www.ic3.cat

001

IMPACT OF INITIAL PERTURBATIONS IN DECADAL PREDICTION

H. Du(1), F.J. Doblas-Reyes(1,2), J. García-Serrano(1),
V. Guémas(1), Y. Soufflet (1), B. Wouters(3)
(1) IC3, (2) ICREA, (3) KNMI

Climate Forecasting Unit
Institut Català de Ciències del Clima

o

12 July 2011

TECHNICAL MEMORANDUM

Series: CFU Technical Memoranda

A full list of CFU Publications can be found on our website under:

http://ic3cfu.wikispot.org

Fundació Institut Català de Ciències del Clima (IC3)
C/ Doctor Trueta, 203 | 08005 Barcelona

Abstract

A coupled global atmosphere-ocean model is employed to investigate the impact of initial perturbation methods on the behaviour of five-member ensemble decadal re-forecasts. Three initial perturbing strategies, which are atmosphere only, ocean only and atmosphere-ocean, have been used and the responses of selected variables have been investigated. The impacts are assessed with respect to climate drift, forecast quality and spread. The simulated global means of near-surface air temperature (T2M), sea surface temperature (SST) and sea ice area (SIA) for both Arctic and Antarctic show reasonably good quality, in spite of the non-negligible drift of the model. The skill is not significantly affected by the particular perturbation method employed. Fast ensemble dispersion can be generated for T2M, SST and land surface precipitation (PCP) in all cases with any of the perturbation methods. However, for SIA, Atlantic meridional overturning circulation (AMOC) and ocean heat content (OHC), the spread increases substantially during the forecast time when oceanic perturbations are applied. Oceanic perturbations are particularly important for Antarctic SIA and OHC for the middle and deep ocean. The results might be helpful in designing ensemble experiments in more efficient ways in which a smaller ensemble size can be used without under-sampling uncertainties for the most useful variables.

1. Introduction

Climate-change projections and near-term climate prediction (also known as decadal prediction) attempt to satisfy a growing demand for climate information for this century. It is well established that, based on knowledge of the initial conditions, important aspects of regional climate are predictable up to a year ahead. Predictability at this time scale is primarily, though not solely, associated with the El Niño Southern Oscillation (ENSO). While climate forecasting is currently addressing the problem of climate prediction up to one year (e.g., Doblas-Reyes et al., 2009; Weisheimer et al., 2009; Hermanson and Sutton, 2010), decadal prediction focuses on time scales of several years to a few decades (e.g., Smith et al., 2007; Meehl et al., 2009).

There have been attempts to predict interannual-to-decadal climate variations using empirical models that take into account persistence of anomalies and/or changes in boundary conditions, i.e. atmospheric composition and solar irradiance (e.g. Lean and Rind, 2009; Hawkins et al., 2011). Others (e.g. Räisänen and Ruokolainen, 2006; Ruokolainen and Räisänen, 2007) have employed the boundary-forced climate projections performed as part of the Third Coupled Model Intercomparison Project (CMIP3; Meehl et al., 2007), from where the part of the simulations corresponding to the first few years of the XXI Century were used to issue a climate prediction for the near term. As a slightly more ambitious alternative, dynamical decadal prediction explores the ability of the type of climate model employed in the Intergovernmental Panel for Climate Change (IPCC) assessments to predict regional climate changes in the near future by exploiting both initial-condition information and changes in boundary conditions. This approach aims to take advantage of the predictability of natural climate variability to make predictions.

For any decadal prediction system, a critical question is to understand how far ahead the mean climate is predictable at regional spatial scales with some useful level of skill and enough reliability. The relative importance of the initial conditions in climate prediction is supposed to vary with the time scale, but has been assumed to be a continuous function that decreases with forecast time, becoming negligible after several decades (Hawkins and Sutton, 2009). For the time scales ranging between a few seasons to a couple of decades, previous work (Smith et al., 2007; Keenlyside et al., 2008; Pohlmann et al., 2009; Mochizuki et al., 2010) has shown evidence that the initial state of the ocean, sea-ice, land and atmosphere can influence climate forecasts a decade or more ahead. In the context of initialized decadal prediction, the question of the extent to which a better knowledge of the initial conditions of the climate system contributes to the quality of these forecasts is related to the way the ensemble is generated to provide reliable forecasts.

The strategy followed for the initialization of the decadal predictions has so far been quite different from that used in seasonal forecasting. For instance, Smith et al. (2007), Pohlmann et al. (2009) and Mochizuki et al. (2010) used the so-called anomaly initialization method, where ocean observations are assimilated in the form of anomalies into the coupled model taking, or not, into account the error covariance of the coupled model. In Keenlyside et al. (2008) only observed sea surface temperature (SST) anomaly information was used to

initialize the coupled system, with no further restrictions in deeper ocean temperature or salinity. In seasonal forecasting, however, it is common practice the separate initialization of the ocean and the atmosphere, data assimilation being used to bring the state of each component of the coupled model close to the observed state. In this study, we use the EC-Earth climate forecast system (Hazeleger et al., 2010) to investigate how the initial-perturbation strategy behaves in a decadal forecasting context. The criteria for the assessment are the extent to which atmospheric and ocean variables are sensitive to the initial-condition perturbations in the forecast range from one to five years, i.e. beyond the generally accepted limit of ENSO-related predictability.

A brief summary of the experiment follows in Section 2. The most relevant characteristics in terms of model drift and forecast quality results are given in Section 3. The differences in the spread of the main climate variables, is described in Section 4 and the main conclusions are summarized in Section 5.

2. Experimental setup

2.1 The forecast system

EC-Earth (Hazeleger et al., 2010) is a coupled atmosphere-ocean model developed by a number of meteorological services and research groups in Europe. Its atmospheric component is a version of IFS which is the operational numerical weather predicting system from the European Centre for Medium-Range Weather Forecast (ECMWF). It has 62 vertical levels and uses a TL159 horizontal resolution. For the oceanic component, NEMO (Nucleus for European Modelling of the Ocean), a state-of-the-art oceanic modelling system from the Institut Pierre-Simon Laplace (IPSL) in France, has been used with the ORCA1 configuration. For sea ice, the Louvain-la-Neuve (LIM2) sea-ice model is directly coupled to NEMO. The atmospheric and ocean components are coupled together via a coupler called OASIS3.

2.2 Experiments

The primary purpose of this study is to investigate the sensitivity of the EC-Earth forecast system to different ways the ensemble is generated. Three ensemble forecast experiments have been performed. The experiments differ from each other by using different sets of initial perturbations. The five-member ensemble re-forecasts start on the first of November every five years over the period 1960 to 2005 and run for 60 months. These starting dates are selected so that they follow the CMIP5 experimental setup (Taylor et al. 2011).

The first experiment only uses atmospheric perturbations (AP). The second experiment starts the five members of each ensemble from one of the NEMOVAR-COMBINE re-analyses (oceanic perturbations; OP). The third experiment uses both atmospheric and oceanic perturbations (OAP).

The atmosphere and land surface initialization was taken from the ERA-40 reanalysis (Uppala et al., 2005) for all start dates before 1989 and ERA-Interim afterwards. The atmospheric perturbations are applied to all members except for the first one and are based on the operational singular vectors (Magnusson et al., 2008). The perturbations are added at the initial time to all the prognostic variables except humidity.

The ocean initial conditions have been taken from the 3D-Var five-member ensemble ocean re-analysis known as NEMOVAR-COMBINE (Balmaseda et al., 2010). The re-analysis has been performed with a variational data assimilation system based on the ocean model NEMO v3.0 where profiles of temperature and salinity from a quality controlled EN3_v2a data set (Ingleby and Huddleston, 2007) were assimilated. The assimilation cycle is 10 days and a bias correction method has been included. The NEMO model is forced by ERA40 fluxes from 1957 to 1988 and by ERA-Interim thereafter (Balmaseda et al. 2010) and includes a strong relaxation to observed SSTs. The reanalysis covers the period of 1958-2009. The five members are generated by perturbing the wind stress, the ocean initial conditions and the subset of observations assimilated. The comparison with independent observations shows that

the assimilation of ocean data helps constraining the uncertainty introduced by ocean models and forcing fluxes, mostly in the upper ocean.

The sea-ice initial conditions are produced from a NEMO v2.0 coupled to LIM2 driven by the DFS4.3 ocean forcing data (Brodeau et al. 2009). This forcing dataset is derived from ERA40/ERAInterim with corrections on tropical surface air humidity, Arctic sea surface temperature and global wind field based on high quality observations. Note that no volcanic aerosol load is applied during the re-forecasts.

3. Drift and forecast quality assessment

3.1 Drift

In full initialization forecast experiments, model inadequacy causes simulations to drift away from the observed climate towards an imperfect model climate. Estimates of the drift, considered as the bias evolution with forecast time, have been computed for the three experiments (OP, AP, OAP) using different reference datasets. The model bias is the difference for a specific forecast time between an estimation of the model and observed mean climates. The subset of modelled and observed data used to estimated the respective climatology is selected following a per-pair method (García-Serrano and Doblas-Reyes 2011)

The global-mean two-metre air temperature (T2M) for the NCEP/NCAR (NCEP/NCAR R1, Kalnay et al. 1996) and ERA-Interim reanalyses shows a mean climate approximately 0.5ºC warmer for the latter than for NCEP/NCAR R1. The ERA data appears to show a larger annual amplitude with higher summer temperature as well. This is due to the different orography used by these reanalyses. The model drift shows a fast cooling during the first two years and a more stable climate during the second half of the integration (Fig. 1a). Land-only globally-averaged T2M displays the same behaviour along the forecast time (not shown). The largest biases in both global and land-only T2M take place during boreal winter (December-to-February) and summer (June-to-August).

The model globally averaged land-only precipitation (PCP) is compared with three observational datasets, GPCC (Rudolf and Schneider 2005), GPCP (Adler et al. 2003) and CRU TS3.0 (Mitchell and Jones 2005) in Figure 1b. The GPCP data obviously have the largest values among these three datasets for the whole period. The CRU values are close to the GPCC values along the whole annual cycle. The model underestimates the PCP along the forecast time, with a slight tendency of the drift towards wetter conditions after the first forecast year. The amplitude of annual cycle of observations is not reproduced.

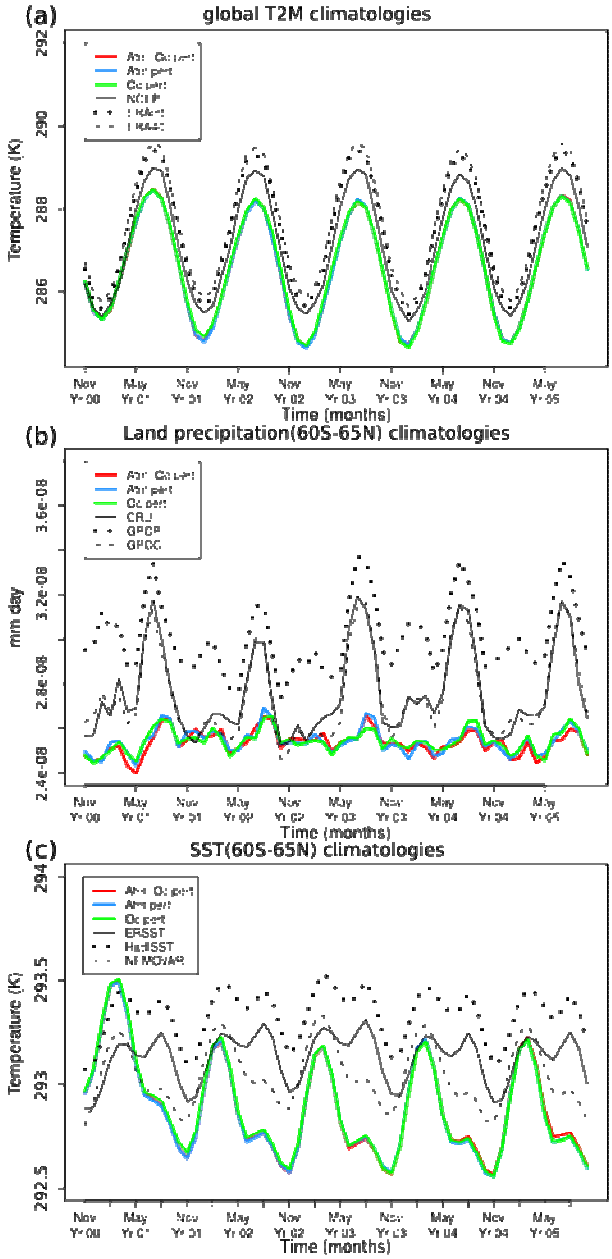

Fig. 1: Evolution of the observational and model climatologies for T2M global-mean (a), global land precipitation averaged over 60°S-65°N (b), and SST averaged over 60°S-65°N (c) along the re-forecasting time, based on monthly means. The climatologies are computed based on the reference period for which both observations and re-forecasts for a specific forecast time are available.

The model sea surface temperature (SST) is compared with three observational datasets, NOAA Extended Reconstructed SST v3b (hereafter ERSST, Smith et al. 2008), HadISST v1.1 from the UK Met Office (hereafter HadISST, Rayner et al. 2003), and the NEMOVAR reanalysis. On average, HadISST yields a 0.2-0.3 K warmer seasonal cycle than ERSST and NEMOVAR, whereas ERSST and NEMOVAR are close during boreal winter and spring (December-to-April) and diverge during summer and autumn (May-to-November). As for T2M, the re-forecast

global-mean (60°S-65°N) SST depicts a cooling drift during the first two forecast years, stabilizing afterwards (Fig. 1c) in agreement with what is found for T2M. There is an initial shock with warm SSTs in the first half of the first forecast year, before the re-forecasts start the cooling drift. Larger SST biases are present during summer and early-winter (July-to-December) than during the rest of the year.

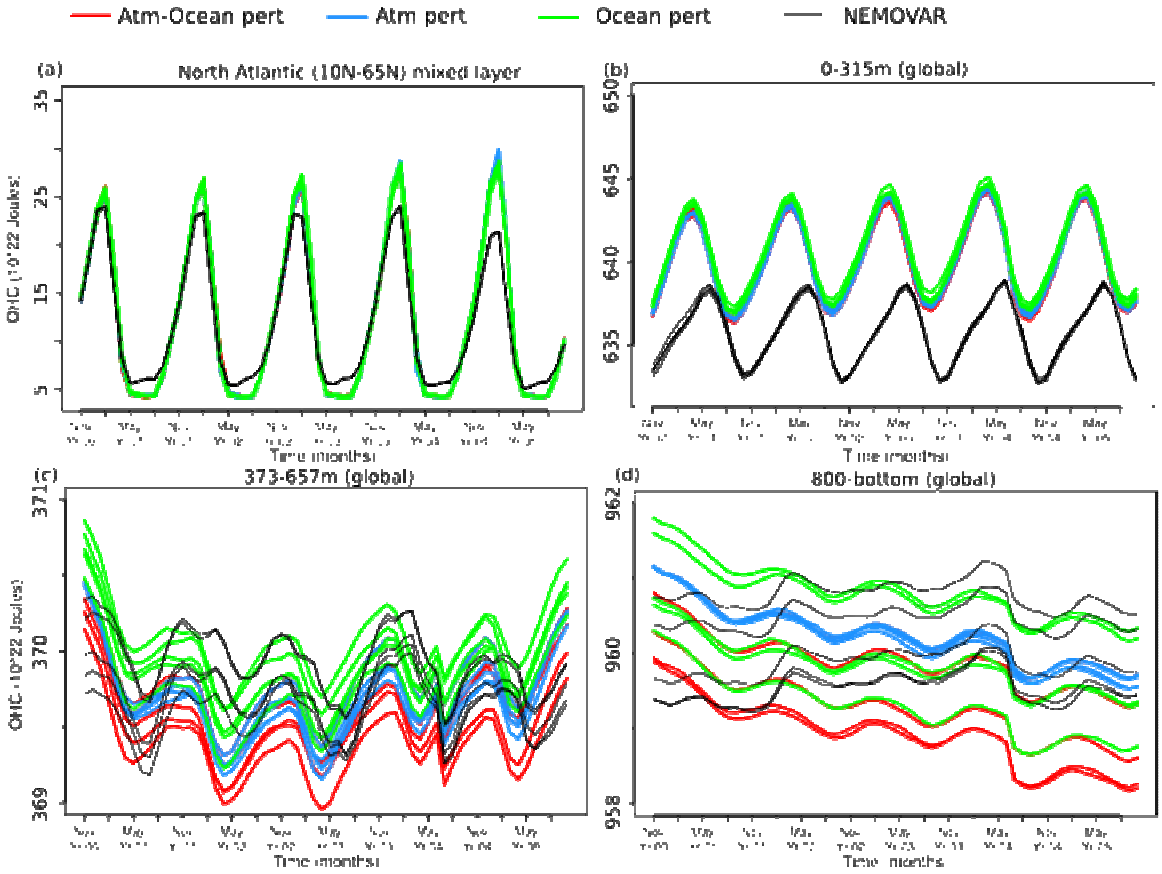

Fig. 2: Evolution of the observational and model climatologies of OHC for mixed layer (a), 0-300m (b), 300-800m (c) and 800-bottom (d) along the forecast time, based on monthly means. The climatologies are computed based on the reference period for which both observations and re-forecasts for a specific forecast time are available.

To assess some aspects of the drift in the ocean, the re-forecast global ocean heat content (OHC) climatology is compared with the NEMOVAR ocean reanalysis. Four different layers have been selected to assess the OHC drift: from the mixed, the upper (0-300m), mid (300-800m) and deep (800-bottom) oceans (Fig. 2). Note that the OHC for mixed layer is only for 10N-65N of Atlantic and OHC for other layers are for global. For mixed layer, warming and cooling drift is found respectively in boreal winter and summer season. Contrary to atmosphere (T2M) and surface ocean (SST) drift, the upper ocean OHC shows a warming with forecast time, while the mid layer shows a fast cooling drift during the first half year of the forecast time and gains heat during the second half of the re-forecast time. A monotonic cooling drift in the deep ocean represents a persistent, pronounced heat flux from the deeper ocean upward to the surface. This feature may explain both the warming drift in the

intermediate layer in the second half of the integration and the heat storage in the upper layer with forecast time.

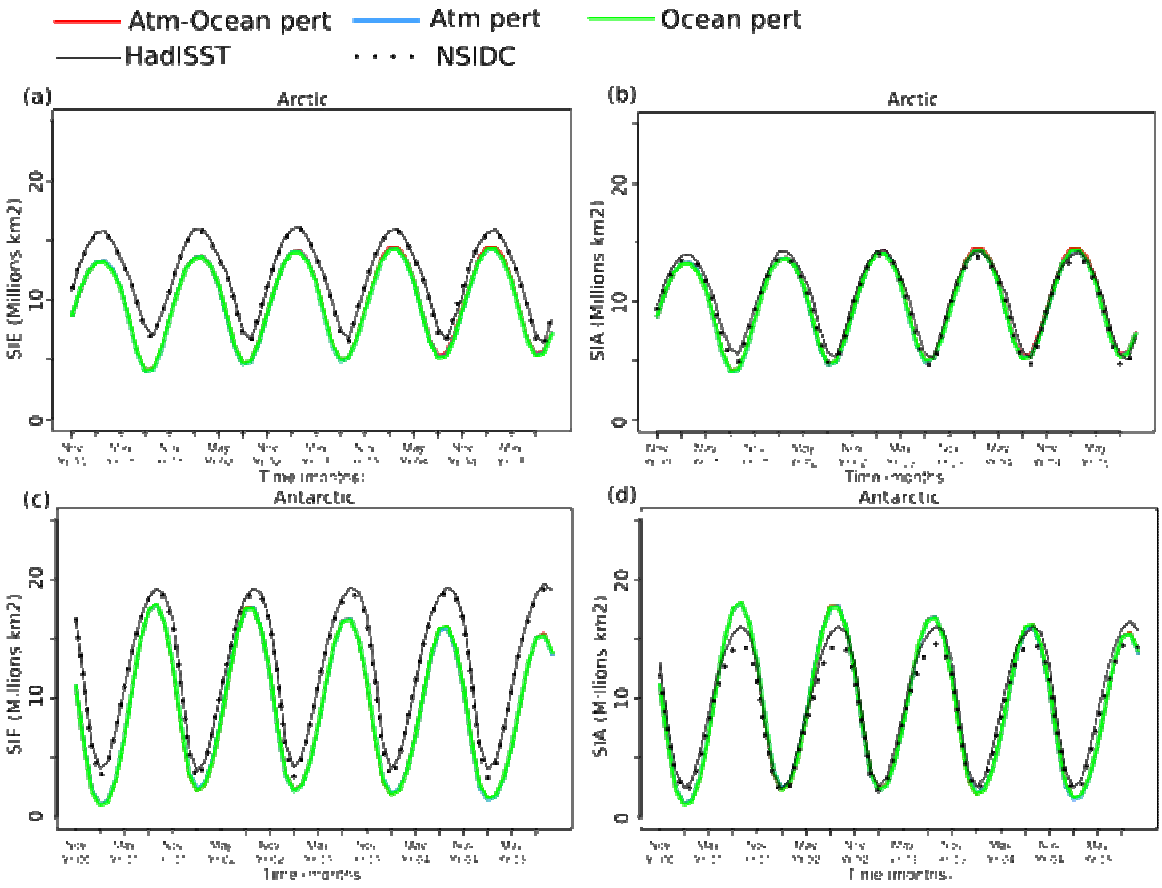

Fig. 3: Same as Fig. 1, but for Arctic Sea ice extent (a), Arctic sea ice area (b), Antarctic sea ice extent (c) and Antarctic sea ice area (d).

For sea ice, sea-ice extent (SIE) and sea-ice area (SIA) are two commonly used variables to assess the performance of models in re-forecasting sea ice. SIE is the area of sea where ice coverage is above a specified threshold, usually 15% (Meier et al. 2007). The model SIE and SIA in the Arctic (Fig. 3a, b) and Antarctic (Fig.3 c and d) is compared with two observational datasets: HadISST (Rayner et al. 2003) and NSIDC (Cavalieri et al. 1996). For these two datasets, the SIE values are close to one another, but SIA values are, on average, larger in HadISST than in NSDIC.

In terms of SIE, the model climatology fits both HadISST and NSIDC seasonal cycle in both Arctic and Antarctic, albeit showing a clear underestimation for all forecast times. EC-Earth shows an increasing trend for Arctic (Fig. 3a) and a decreasing trend for Antarctic (Fig. 3c) over the whole reforecast periods and depicts larger extent during late summer and late winter. With respect to SIA, Arctic shows a negative drift in the first two reforecast years and starts to recover afterwards. Antarctic SIA depicts negative drift in late winter and positive drift in late summer and becomes stabilized afterwards. There is also an initial shock towards lower Antarctic SIE values during the first boreal winter in the forecast.

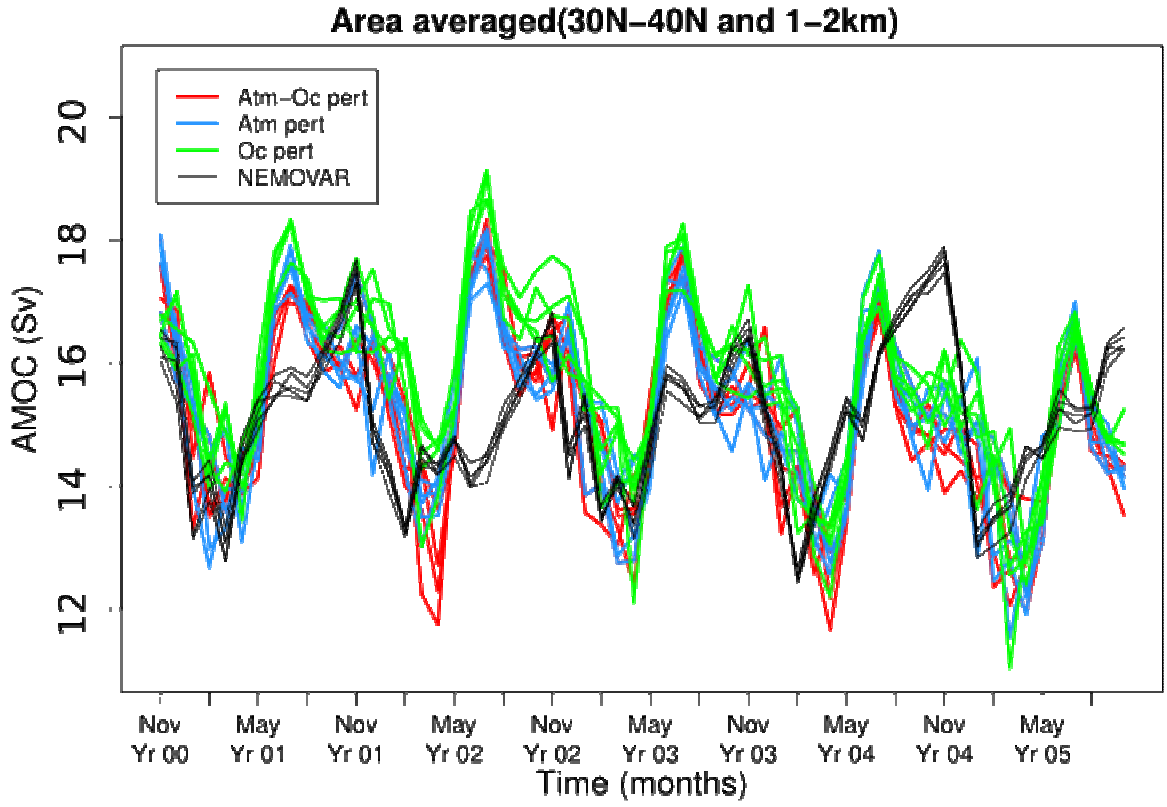

Fig. 4: Same as Fig. 2, but for Area averaged AMOC (30N-40N and 1-2km deep).

The EC-Earth systematic error in the Atlantic meridional overturning circulation (AMOC) has also been evaluated and compared to estimates from the NEMOVAR reanalysis (Fig. 4). The area averaged (30N-40N and 1-2km deep) AMOC shows a similar magnitude compared to the observations. However, they are not consistent in terms of seasonal variations. It also depicts a slightly decreasing trend with lead time.

3.2 Forecast quality assessment

To assess the quality of the predictions, correlation between the bias-corrected ensemble-mean predictions and the available observations have been estimated. All monthly anomalies are calculated by subtracting the monthly climatology. Statistical significance is assessed using a two-tailed Student's t-test for correlation at the 95% confidence level.

Figure 5a shows the correlation between the three experiments and the two sets of observed T2M, NCEP/NCAR R1 and ERAInterim. The re-forecasts show a good agreement with NCEP/NCAR R1, but bad performance with respect to ERAInterim. This is partly due to the different periods used to compute the correlation, NCEP having a much longer record than ERAInterim. When the correlation for NCEP/NCAR R1 is computed based on the same period as the ERAInterim the results also show a low correlation (not shown). One of the main failures of this set of re-forecasts is the underprediction of the effects of the Agung, El Chichon and Pinatubo eruptions and the typical lack of skill to predict the ENSO events (in

particular the one occurred in 1997-1999) beyond the second year of the forecast. These effects are particularly noticeable in small samples such as the one used in the verification against ERAInt (García-Serrano and Doblas-Reyes 2011).

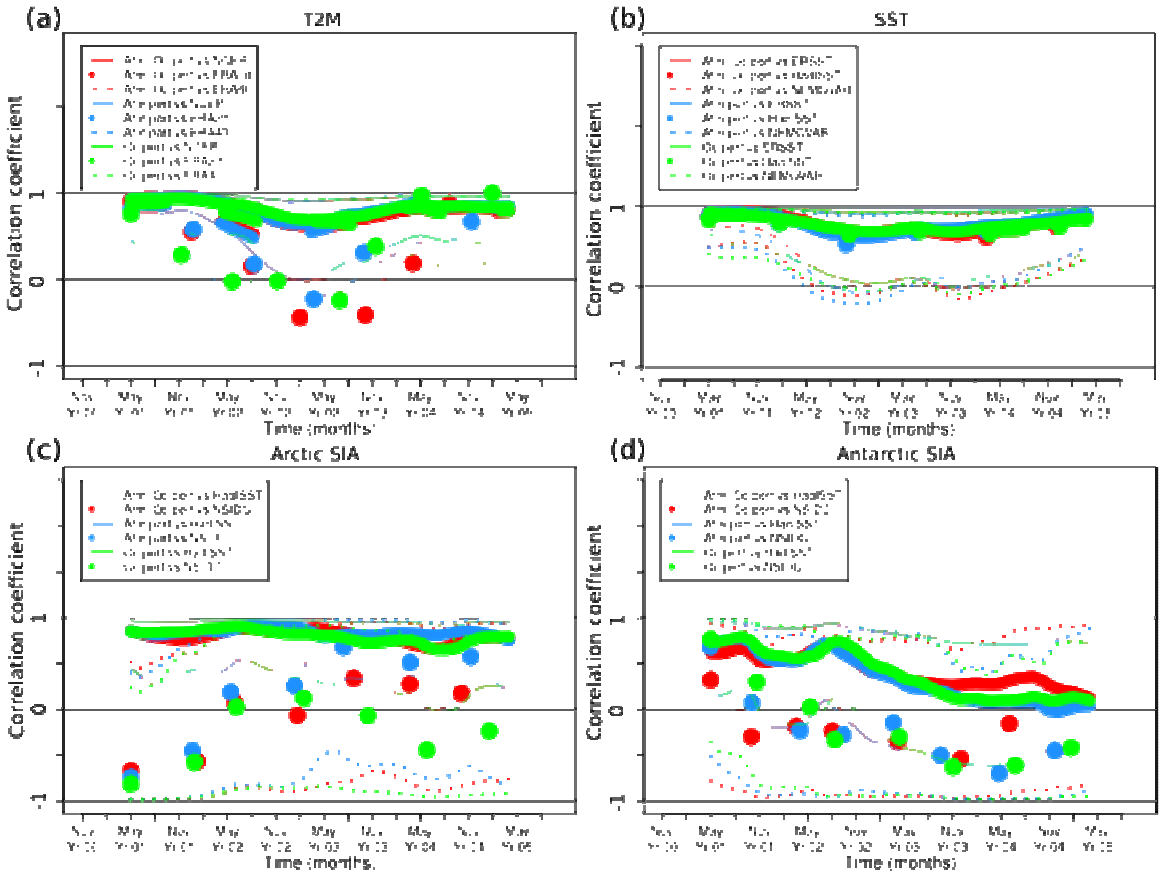

Fig. 5: Anomaly correlation coefficient (ACC) for T2M (a), SST (b) and sea ice area for Arctic (c) and Antarctic (d) between each experiment and different observational data. The correlations are computed based on the reference period for which both observations and re-forecasts for a specific forecast time are available. Anomalies have been smoothed based on 12-month running average. Confidence intervals (α<0.05) for correlations are drawn between thin lines.

Figure 5b shows the correlation for a global-mean estimate of the SST. The re-forecasts show a good skill compared to all three observational datasets. Similar to T2M, the correlation in the middle of the re-forecasting period is relatively weak. This might be also due to the failure in re-forecasting the strong ENSO events of 1997-1999.

Figure 5c and 5d depict the correlation for SIA of Arctic and Antarctic respectively. The model results also show a good skill compared to HadISST , but not with NSIDC. This is also due to the relatively short record for NSIDC, which results from under-sampling of data. The model shows some skill in the first two leading years compared to HadISST for the Antarctic and the performance rapidly decreases afterwards. When only the data of HadISST after 1978 are used, the model does not show correlation either (not shown).

For precipitation, OHC, and maximum, latitude and depth of AMOC, no statistically significant correlation have been found (not shown). For OHC and AMOC, this is not surprising because huge uncertainties exist in the ocean initial conditions due to lack of observations before 1980s. For precipitation, numerical models usually do not have much skill.

4 Spread

The distance between the maximum and the minimum ensemble member averaged across all starting dates is used to characterize the ensemble spread because more traditional methods, such as the standard deviation around the ensemble mean will give a less robust estimate with such small sample size (five values). Unlike the forecast quality assessment, statistical significance with a confidence level of 0.95 for the spread is estimated using a non-parametric bootstrap test due to the limited ensemble members.

Figure 6a shows the range between the maximum and minimum T2M (maximum minus minimum) across the five ensemble members of the AP, OP and AOP experiments. After about one year, a large spread has been generated in all cases, although the spread seems to grow faster when oceanic perturbations are used. Either AP or OP seems to be adequate to sample the initial-condition uncertainties.

Figure 6b shows a similar analysis for SST. Similar to T2M, the spread the three experiments produce is close to each other. An interesting feature is that, in the last couple of months, it seems that OP is driving a larger dispersion compared to AP and AOP. It might be useful to have some longer runs to check how this feature evolves with the forecast time.

For land-only precipitation (Figure 6c), the spread is generated earlier (in half year) compared to T2M and SST. No initial-perturbation methods show dominance in producing a larger spread.

Figure 6d and 6e display the effect of the initial perturbations on the spread of SIA over the Arctic and Antarctic regions. The spread increases with the forecast time in all cases for the Arctic. A slight superiority to generate a larger spread is found for OP in the first three years. For Arctic, the spread also increases with forecast time over the Antarctic and OP shows a systematic larger dispersion.

With respect to AMOC, Figure 6f shows the spread for the area averaged AMOC (30-40N and 1-2km deep). Perturbation methods do not seem to show obvious influences in the first two years. However, atmospheric perturbations seem to be more important and produce more spread after four years.

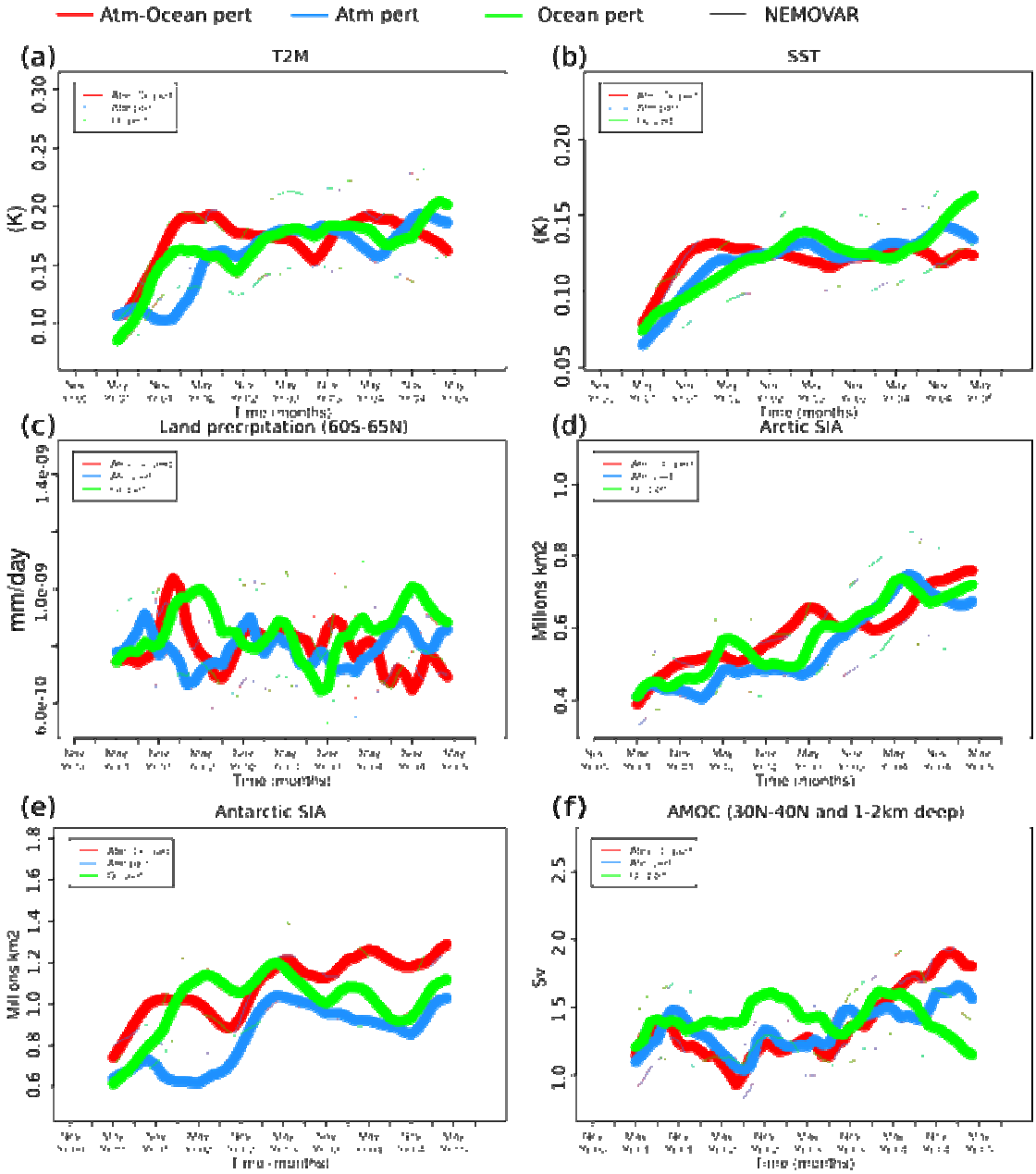

Fig. 6: Ensemble maximum minus Ensemble minimum of smoothed anomaly climatologies of each member with 95% confidence interval (between the thin lines) for T2m (a), SST (b), Precipitation (c), Arctic SIA (d), Antarctic SIA (e) and AMOC (f). Anomalies for each member, which are used to compute the 'maximum minus minimum', have been smoothed based on 12-month running average. The statistical significance for the spread is estimated using a non-parametric bootstrap test.

Figure 7a, 7b, 7c and 7d show the spread for global OHC of the mixed, the top (0-300m), middle (300-800m) and lower (800-bottom) layers. In all four layers, the magnitude of the spread increases with the evolution of forecasting time. For mixed layer, three perturbation methods produce similar magnitudes of dispersion. However, it seems that AP produces less spread in late summers compared to OP and AOP. For the top layer, AP has an almost linearly

increasing spread, but it produces a magnitude of spread similar to the experiments with OP in the last forecast year. For the middle and bottom layers, OP produces systematically more spread than AP. This is mainly because of the large observational uncertainties introduced in the NEMOVAR ocean reanalysis.

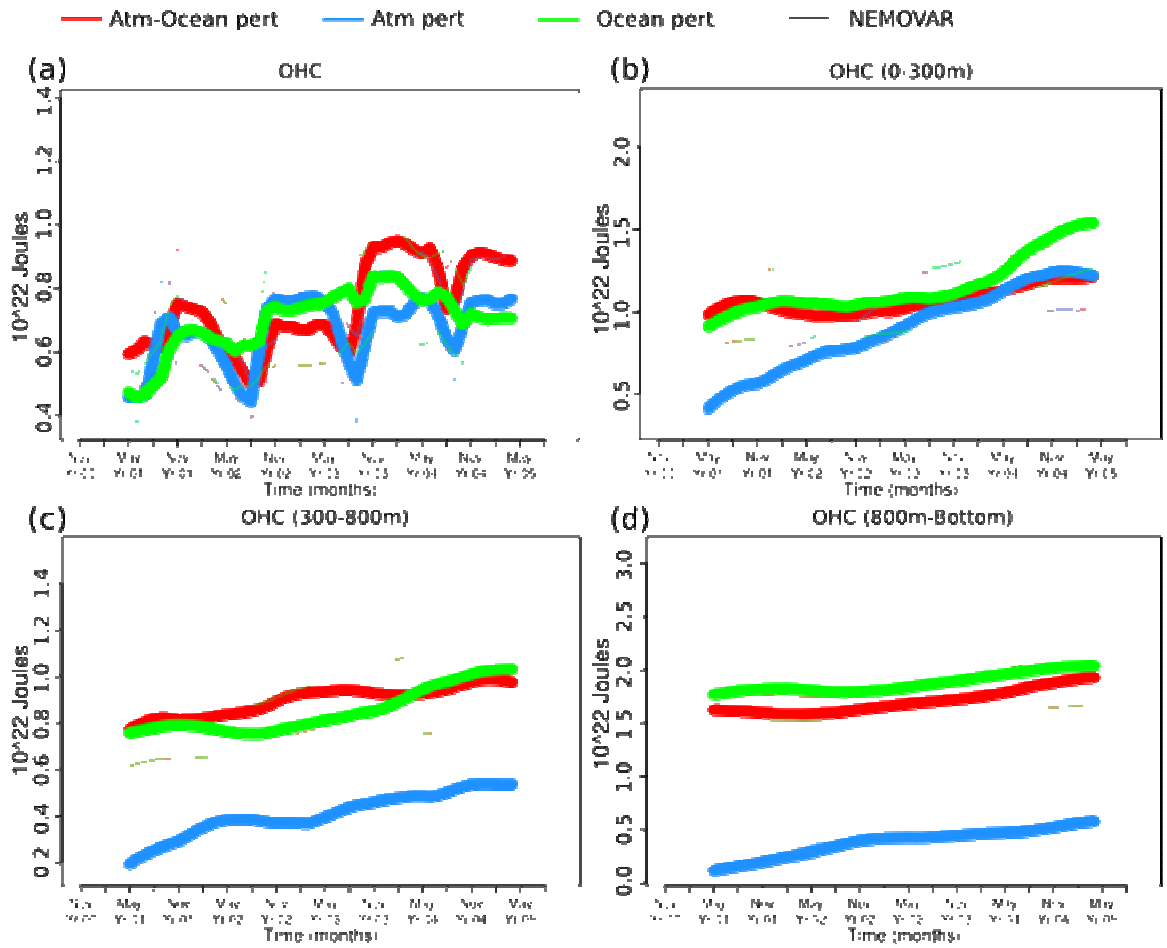

Fig. 7: Same as Fig. 6 but for OHC of mixed layer (a), OHC of 0-300m (b), OHC 300-800m (c) and OHC 800-bottom (d).

5. Conclusions

Different perturbation strategies are employed to investigate the responses from the EC-Earth forecast system in our study in a decadal prediction context. The forecast system was initialized using the best estimates of the observed climate, which is known as full initialization. Three different five-member ensemble experiments were carried out with perturbations in the atmospheric component only, in the oceanic component only and in both.

The particular initial perturbation method does not affect how the re-forecasts drift away from the observed climate or their correspondence to the observations, which has been

measured using the difference between the model climatology and the corresponding observational climatology. For most atmospheric variables, climate drift usually happens in the first 1-2 years and stabilizes afterwards. T2M and SST show a cold drift. The global-mean land precipitation is underestimated and shows less variability than the observations, in particular, the maximum values of the inter-annual changes are not well captured. OHC in several layers and AMOC also show some substantial drift, especially for OHC which shows a warmer top layer and colder deep layer, indicating that the heat exchange between different levels of the ocean are not well represented.

The forecast quality estimates suffer from the short samples typically used in decadal forecasting. For short records, error intervals for forecast quality estimates are very large. In addition to this, it is important to take into account the approach used to estimate the observed climatology.

The paper tries to address two main questions about ensemble spread in decadal prediction. First, it analyzes how the predictions react to different perturbation methods. Second, it estimates the rate at which the spread is generated, measured as the spread evolution with the forecast time.

For T2M, precipitation, SST, a similar spread is generated in all cases, which means that the spread is not determined by only atmospheric or oceanic perturbations. For sea ice, EC-Earth shows different behaviour for the Arctic and the Antarctic. Arctic sea ice is not sensitive to the way in which the initial conditions are perturbed, while oceanic perturbations are fundamental to generate spread for Antarctic sea-ice area. The oceanic perturbations are also critical to produce enough spread for the OHC, except when diagnosed for the mixed layer. The oceanic perturbations are necessary to take into account the lack of observations in the deep ocean, which is sampled with a large spread of the ocean initial conditions taken from NEMOVAR. The averaged AMOC over 30-40ºN and 1-2 km shows a slightly different behaviour because while oceanic perturbations are important in the first half of the forecast, atmospheric perturbations are as important afterwards.

The spread is generated at a fast rate for T2M, SST and precipitation while for the ocean variables the spread increases over the whole forecast time. Hawkins and Sutton (2009) investigated the growth of Atlantic ocean anomalies by using climatology singular vector to generate perturbations for three-dimensional ocean temperature and salinity. Their results show that growth of optimal perturbations with the lead time can occur in time scales longer than 10 years. In our study, although we use a different perturbation method for the ocean, OHC and SIA spread seems to be growing continuously over the full forecast period. This suggests that longer simulation might be required for better understanding the amplification of the perturbations for some ocean and sea-ice variables with forecast time.

In summary, while the spread for atmospheric variables like T2M, SST and precipitation grows at a similar rate with any perturbation method, most of the ocean-related variables are more sensitive to the oceanic perturbations. In the context of initialized decadal forecasting being carried out with multiple forecast systems, some of them not having a way to perturb the

ocean initial conditions, it is useful to learn that atmospheric perturbations can generate enough spread for many useful variables, including in the ocean such as the SSTs and the AMOC.

Acknowledgement

This work was supported by the EU-funded QWeCI (FP7-ENV-2009-1-243964) and the MICINN-funded RUCSS (CGL2010-20657) projects. The authors thankfully acknowledge the computer resources, technical expertise and assistance provided by the Red Española de Supercomputación (RES).

References

Adler, R. F., G. J. Huffman, A. Chang, R. Ferraro, P. Xie, J. Janowiak, B. Rudolf, U. Schneider, S. Curtis, D. Bolvin, A. Gruber, J. Susskind, P. Arkin, and E. Nelkin (2003), The version 2 vlobal precipitation climatology project (GPCP) monthly precipitation analysis (1979-present), J. Hydrometeor 4:1147-1167.

Balmaseda, M.A., K. Mogensen, F. Moteni and A.T weaver (2010) The NEMOVAR-COMBINE ocean re-analysis. NEMOVAR Technical reports No. 1. http://www.combine-project.eu/Technical-Reports.1668.0.html

Brodeau L. Bernard Barnier, Anne-Marie Treguier, Thierry Penduff, Sergei Gulev (2009) An ERA40-based atmospheric forcing for global ocean circulation models. Ocean Modelling 31:88-104. doi:10.1016/j.ocemod.2009.10.005 Key: citeulike:6067348

Cavalieri, D., C. Parkinson, P. Gloersen, and H. J. Zwally (1996) Sea Ice Concentrations from Nimbus-7 SMMR and DMSP SSM/I Passive Microwave Data, [list dates of temporal coverage used]. Boulder, Colorado USA: National Snow and Ice Data Center. Digital media.

Doblas-Reyes, F. J., A. Weisheimer, M. Déqué, N. Keenlyside, M. McVean, J. M. Murphy, P. Rogel, D. Smith, and T. N. Palmer (2009) Addressing model uncertainty in seasonal and annual dynamical seasonal forecasts. Quart J Roy Meteor Soc 135. doi:10.1002/qj.464.

García-Serrano, J. and F. J. Doblas-Reyes (2011) On the assessment of near-surface global temperature and North Atlantic multi-decadal variability in the ENSEMBLES decadal hindcast. Clim. Dyn. (submitted)

Hawkins, E., and R. Sutton (2009) The potential to narrow uncertainty in regional climate predictions. Bull Amer Meteor Soc 90:1095-1107. doi: 10.1175/2009BAMS2607.1

Hawkins, E., J. Robson, R. Sutton, D. Smith and N. Keenlyside (2011) Evaluating the potential for statistical decadal predictions of sea surface temperature with a perfect model approach. Climate Dyn. doi: 10.1007/s00382-011-1023-3

Hermanson, L., and R. T. Sutton (2009) Climate predictability in the second year. Phil. Trans. R. Soc. A, 367:913-916

Ingleby, B., and M. Huddleston (2007) Quality control of ocean temperature and salinity profiles - historical and real-time data. Journal of Marine Systems 65:158-175

Kalnay, E., M. Kanamitsu, R. Kistler, W. Collins, D. Deaven, L. Gandin, M. Iredell, S. Saha, G. White, J. Woollen, Y. Zhu, M. Chelliah, W. Ebisuzaki, W. Higgins, J. Janowiak, K. C. Mo, C. Ropelewski, J. Wang, A. Leetmaa, R. Reynolds, R. Jenne, D. Joseph (1996) The NCEP/NCAR 40-year reanalysis project. Bull Amer Meteor Soc 77:437-470

Keenlyside N. S, M. Latif, J. Jungclaus, L. Kornblueh, and E. Roeckner (2008) Advancing decadal-scale climate prediction in the North Atlantic sector. Nature 453:84–88. doi:10.1038/nature06921

Lean, J. L., and D. H. Rind (2009) How will Earth's surface temperature change in future decades. Geophys Res Lett 36:L15708. doi:10.1029/2009GL038932

Magnusson, L., M. Leutbecher and E. Kallen (2008) Comparison between singular vectors and breeding vectors as initial perturbations for the ECMWF Ensemble Prediction System. Mon Wea Rev 134:4092-4104

Meehl, G. A., C. Covey, T. Delworth, M. Latif, B. McAvaney, J. F. B. Mitchell, R. J. Stouffer, and K. E. Taylor (2007) The WCRP CMIP3 multi-model dataset: A new era in climate change research. Bull Amer Meteor Soc 88:1383-1394

Meehl, G. A., L. Goddard, J. Murphy, R. J. Stouffer, G. Boer, G. Danabasoglu, K. Dixon, M. A. Giorgetta, A.M. Greene, E. Hawkins, G. Hegerl, D. Karoly, N. Keenlyside, M. Kimoto, B. Kirtman, A. Navarra, R. Pulwarty, D. Smith, D. Stammer, and T. Stockdale (2009) Decadal prediction, can it be skillful? Bull Amer Meteor Soc 90:1467-1485. doi: 10.1175/2009BAMS2778.1

Meier, W. N., J. Stroeve, and F. Fetterer (2007) Whither Arctic sea ice? A clear signal of decline regionally, seasonally, and extending beyond the satellite record. Annals of Glaciology 46:428-434. doi:10.3189/172756407782871170

Mitchell, T. D. and P. D. Jones (2005) An improved method of constructing a database of monthly climate observations and associated high-resolution grids. Int J Clim 25:693-712

Mochizuki, T., M. Ishii, M. Kimoto, Y. Chikamoto, M. Watanabe, T. Nozawa, T. T. Sakamoto, H. Shiogama, T. Awaji, N. Sugiura, T. Toyoda, S. Yasunaka, H. Tatebe, and M. Mori (2010) Pacific decadal oscillation hindcasts relevant to near-term climate prediction. PNAS 107:1833-1837. doi: 10.1073/pnas.0906531107

Pohlmann, H., J. H. Jungclaus, A. Köhl, D. Stammer, and J. Marotzke (2009) Initializing decadal climate predictions with the GECCO oceanic synthesis: Effects on the North Atlantic. J Climate 22:3926-3938

Räisäinen, J., and L. Ruokolainen (2006) Probabilistic forecasts of near-term climate change based on a resampling ensemble technique. Tellus A, 58:461–472. doi: 10.1111/j.1600-0870.2006.00189.x

Rayner, N. A., D. E. Parker, E. B. Horton, C. K. Folland, L. V. Alexander, D. P. Rowell, E. C. Kent, A. Kaplan (2003) Global analyses of sea surface temperature, sea ice, and night marine air temperature since the late nineteenth century. J Geophys Res 108 D14. doi:10.1029/2002JD002670

Rudolf, B. and U. Schneider (2005) Calculation of Gridded Precipitation Data for the Global Land-Surface using in-situ Gauge Observations. Proceedings of the 2nd Workshop of the International Precipitation Working Group IPWG, Monterey October 2004, EUMETSAT, ISBN 92-9110-070-6, ISSN 1727-432X, 231-247

Ruokolainen, L. and J. Räisäinen (2007) Probabilistic forecasts of near-term climate change: sensitivity to adjustment of simulated variability and choice of baseline period. Tellus A, 59A:309-320. doi: 10.1111/j.1600-0870.2007.00233.x

Smith D. M, S. Cusack, A. W. Colman, C. K. Folland, G. R. Harris, and J. M. Murphy (2007) Improved surface temperature prediction for the coming decade from a global climate model. Science 317:796–799. doi:10.1126/science.1139540

Smith, T. M., R. W. Reynolds, T. C. Peterson, J. Lawrimore (2008) Improvements to NOAA's historical merged land-ocean surface temperature analysis (1880-2006). J Clim 21:2283-2296

Taylor K.E., R.J. Stouffer, G. A. Meehl (2011) A Summary of the CMIP5 Experiment Design. Available from http://cmip-pcmdi.llnl.gov/cmip5/docs/Taylor_CMIP5_design.pdf.

Uppala, S. M., and 45 others (2005) The ERA-40 reanalysis. Q J R Meteorol Soc 131:2961-3012

Weisheimer, A., F. J. Doblas-Reyes, T. N. Palmer, A. Alessandri, A. Arribas, M. Déqué, N. Keenlyside, M. MacVean, A. Navarra, and P. Rogel (2009) ENSEMBLES - a new multi-model ensemble for seasonal-to-annual predictions: Skill and progress beyond DEMETER in forecasting tropical Pacific SSTs. Geophys Res Lett 36 L21711. doi: 10.1029/2009GL040896

Hazeleger Wilco, Camiel Severijns, Tido Semmler, Simona Ştefănescu, Shuting Yang, Xueli Wang, Klaus Wyser, Emanuel Dutra, José M. Baldasano, Richard Bintanja, Philippe Bougeault, Rodrigo Caballero, Annica M. L. Ekman, Jens H. Christensen, Bart van den Hurk, Pedro Jimenez, Colin Jones, Per Kållberg, Torben Koenigk, Ray McGrath, Pedro Miranda, Twan Van Noije, Tim Palmer, José A. Parodi, Torben Schmith, Frank Selten, Trude Storelvmo, Andreas Sterl, Honoré Tapamo, Martin Vancoppenolle, Pedro Viterbo, Ulrika Willén 2010 EC-Earth: A Seamless Earth-System Prediction Approach in Action. Bulletin of the American Meteorological Society 91(10): 1357-1363. doi: 10.1175/2010BAMS2877.1